Gravity Data Base Generation and Geoid Model Estimation Using Heterogeneous Data

G.S. Vergos✉, I.N. Tziavos, V.D. Andritsanos
Department of Geodesy and Surveying, Aristotle University of Thessaloniki, University Box 440, 541 24, Thessaloniki, Greece, Fax: +30 31 0995948, E-mail: vergos@topo.auth.gr.

Abstract. The computation of high-resolution and high-precision geoid models in the Eastern part of the Mediterranean Sea usually suffers from the few gravity observations available. In the frame of the EU-sponsored GAVDOS project, a systematic attempt has been made to collect all available gravity data for an area located in the Southern part of Greece and determine new and high-resolution geoid models. Thus, all available gravity data have been collected for both land and marine regions and an editing/blunder-removal processing scheme has been followed to generate an optimal gravity dataset for use in geoid determination. The basic analysis and validation of the gravity databank was based on a gross-error detection visualization and collocation scheme. The Least Squares Collocation (LSC) method was employed to predict gravity at known stations and then validate the observations and detect blunders. The finally generated gravity database presents a resolution of 1 arcmin in both latitude and longitude while its external and internal accuracies were estimated to about ±5 mGal and ±0.2 – ±0.4 mGal, respectively. Based on the derived gravity database a gravimetric geoid model was developed using the well-known remove-compute-restore method with an application of a 1D Fast Fourier Transform (FFT) to evaluate Stokes' integral. Altimetric geoid solutions have been also determined from the GEOSAT and ERS1 geodetic mission altimetry data. Finally, combined geoid models have been computed using the FFT-based Input Output System Theory (IOST) and the LSC methods. The consistency of the geoid models estimated was assessed by comparing the geoid height value at the Gavdos Tide Gauge (TG) station on the isle of Gavdos. Their accuracy was determined through comparisons with stacked T/P sea surface heights. From the comparisons performed it was found that the accuracy of the gravimetric, altimetric and combined models was at the ±14.5 cm, ±8.6 cm and ±12.5 cm level, and their consistency at about ±2 cm.

Keywords. Gravity database, least squares collocation, geoid.

1 Introduction

The determination and availability of a high-resolution and high-accuracy geoid model is nowadays a necessity in a large number of geo-sciences, since it serves as the reference surface where other measurements and phenomena of the Earth system are related. This paper summarizes the results obtained during the last two years towards the generation of a consistent and accurate gravity database for Southern Greece and the estimation of a high-accuracy and high-resolution geoid model in support of the EU funded GAVDOS project. GAVDOS project focuses on the establishment of a sea level monitoring and altimeter calibration site on the isle of Gavdos, Greece. To achieve the objectives of the project, the estimation of a geoid model was necessary to serve as a reference surface for the oceanographic, sea level monitoring, tectonic and other studies. Our group was responsible for the collection of all available gravity data for the area under study and the estimation of gravimetric and combined, with altimetric Sea Surface Heights (SSHs), geoid models. The structure of the procedure followed can be summarized as: a) collection and unification of all available gravity data, b) blunder removal and editing, c) gravity database generation and gravimetric geoid model estimation, d) combination of heterogeneous data to estimate a combined geoid model.

2 Gravity database generation

2.1 Gravity data collection

For the generation of the gravity database a total number of 103289 point and mean gravity data were collected from different data sources. Various databases including absolute gravity measurements, relative marine, land and airborne observations were collected for the area of Gavdos bounded between $33° \leq \varphi \leq 38°$ and $20° \leq \lambda \leq 28°$. The distribution of the gravity data is presented in Figure 1.

The entire database was divided into separate files and the observations were encoded according to their origin. In addition, they were reformulated in the classical format of "station ID, latitude, longitude, height and observation". The original databases used were: a) 33560 point marine and land free-air gravity anomalies collected during international campaigns and international projects (Andritsanos and Tziavos 2002; Casten and Makris 2001; Lagios et al. 1996), b) 9322 marine free-air gravity anomalies derived from satellite altimetry (Andersen and Knudsen 1998), which were basically used to fill several gaps in the Eastern Mediterranean Sea, c) 21372 marine free-air gravity anomalies from GEODAS (NGS 2001), d) 1680 airborne free-air gravity anomalies from the CAATER, and e) 39647

marine gravity data from the digitisation of Morelli's maps (Behrend et al. 1996). All observation were referred to IGSN71, the gravity anomalies were computed using the International Gravity Formula of 1980 for the normal gravity and the geographical coordinates were transformed to the GRS80 ellipsoid.

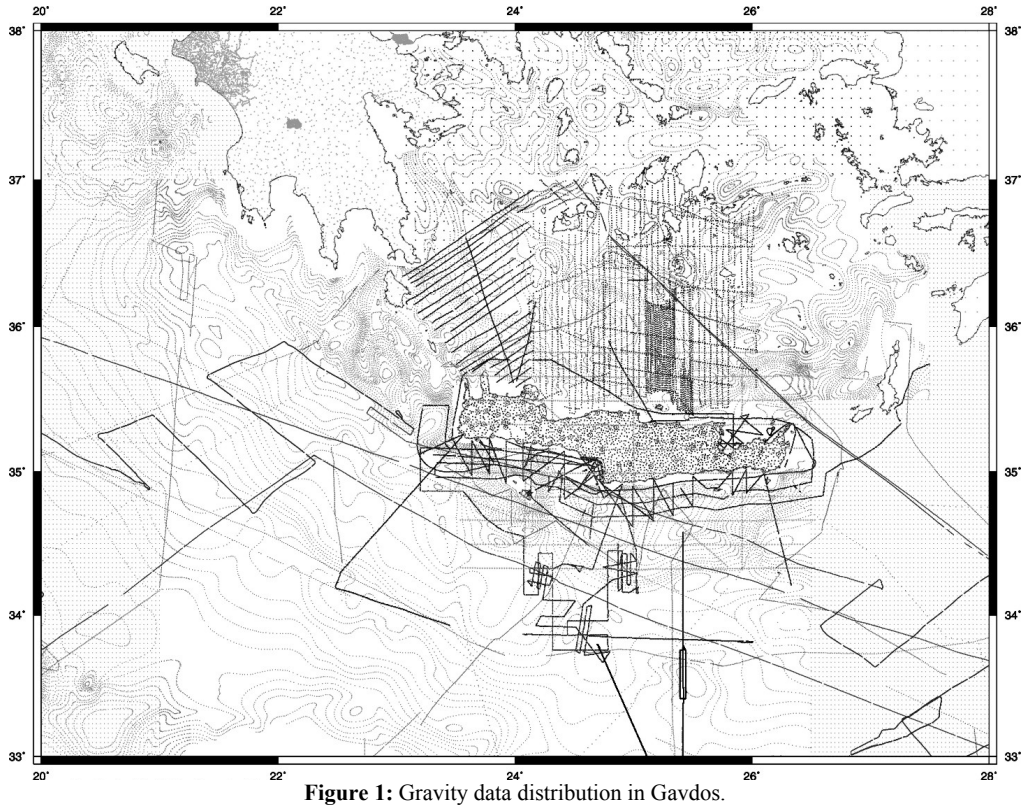

Figure 1: Gravity data distribution in Gavdos.

2.2 Methodology for blunder detection

For the identification and removal of blunders a two-step procedure was followed, i.e., a) visual inspection and b) least-squares collocation.

Taking into account that data related to the gravity field are spatially correlated, gravity quantities of the same type and not far apart will be very similar. Especially, after the removal of a highly expanded geopotential model and of the effect of the neighboring masses, the distribution of the data should be close to normal. According to BGI (1992) an effective check can be done by 2D contouring the data. Thus, following this method, a map of residual, i.e., EGM (Earth Gravity Model) and topographically reduced gravity anomalies, was generated and deep holes and steep spikes were considered to indicate suspicious observations. Since the smoothness of the field is the highest one after the removal of high and low frequency information, large discrepancies can be identified as blunders.

Least squares collocation (LSC) was also used to remove any existing outliers that were not removed during the preceding visual check. A gravity anomaly y was predicted from a set of values x, in neighboring points, spaced as evenly as possible in all directions according to the well-known collocation formula (Tscherning 1991)

$$\tilde{\mathrm{y}} = \mathbf{C}_{\mathrm{y}}\bar{\mathbf{C}}^{-1}\mathbf{x} \tag{1}$$

where $\boldsymbol{C_y}$ is the vector of covariances between y and the x_i values and $\bar{\mathbf{C}} = \mathbf{C} + \mathbf{D}$ is the sum of the covariance matrix of the x_i quantities and the variance-covariance matrix of the noise (error) associated with the quantities. An error estimate was also computed for the difference $|\mathrm{y} - \tilde{\mathrm{y}}|$ as

$$\sigma^2\left(\mathrm{y} - \tilde{\mathrm{y}}\right) = \mathrm{C}_{\mathrm{o}} - \mathbf{C}_{\mathrm{y}}^{\mathrm{T}}\bar{\mathbf{C}}^{-1}\mathbf{C}_{\mathrm{y}} \tag{2}$$

where C_o is the variance of the gravity values. A gross-error was then detected when

$$\left|\mathrm{y}_{\mathrm{obs}} - \tilde{\mathrm{y}}\right| > \mathrm{k}\sqrt{\sigma^2\left(\mathrm{y} - \tilde{\mathrm{y}}\right) + \sigma_{\mathrm{y}}^2} \tag{3}$$

where k is a constant generally having the value 3 to 5 depending on the check strictness and σ_{y}^2 is the error variance of the observation y_{obs}. From the above equations it is obvious that gross-errors are most easily found if C_o is as small as possible. Thus it is obvious that the removal of the long and short wavelengths of

the gravity field is necessary for the outlier detection to lead to rigorous results.

2.3 Results of validation

2.3.1 *Visual inspection*

The total number of free-air gravity anomalies were collected and reformulated in a single file giving as station number a characteristic code for each dataset, so they could be distinguished at a later step. This set formulated the initial set of point free-air gravity anomalies which were then used for the construction of the GAVDOS project gravity database. For the visual inspection, the contribution of the GPM98b EGM (Wenzel 1999) was removed from the raw data while the topographic effects were taken into account through a simple Bouguer reduction. The statistics of the reduced gravity anomalies are presented in Table 1.

Table 1. Statistics of point Δg_f before and after the reduction to GPM98b; Bouguer gravity anomalies (Δg_B) before and after the visual inspection test. Unit: [mGal].

	max	min	mean	σ
Δg_f	270.60	-247.76	-34.46	±82.27
$\Delta g_{f\ red}$	149.03	-111.87	-2.83	±14.34
Δg_B **(before)**	159.74	-247.76	-36.52	±80.41
Δg_B **(after)**	122.40	-136.93	-4.89	±80.38

Employing the so-derived reduced anomaly field, a contour map of the area was generated. Some outliers were identified considering that spikes and holes in the gravity field do not describe local irregularities since the main topographic signal from a Bouguer plate was removed. After this visual inspection test, 94 gravity anomaly observations have been identified as blunders and were subsequently removed from the global database.

2.3.2 Collocation scheme

The procedure described in the previous section was followed to eliminate any existing gross-errors that passed the visual inspection test. Due to the large number of observations, the area under study was divided in 20 sectors of 1°×2° in latitude and longitude each. That was necessary in order to be able to handle the large amount of data and preserve the homogeneity of the field. The total number of observations in each compartment was then divided in two files with equal and homogeneously distributed data points. The data were then reduced to the EGM96 geopotential model and an empirical covariance function was computed and fitted to the Tscherning and Rapp (1974) analytical model from the observations of the first data file. Using the parameters of this model, predictions at the locations of the points of the second file were then estimated. Due to the unavailability of proper measurement error and the ambiguous quality of the data, an error of ±5 mGal was assigned to each observation. A rejection criterion with a parameter k=2 was followed, which was stricter compared to that used in earlier studies (Vergos et al. 2003), so as to remove more suspicious observations and generate a more accurate gravity database. This parameter in conjunction with the overestimated σ of the observations ensured the removal of the largest blunders. A total number of 5729 points were rejected as suspicious gross-errors. The points removed represent a 5.6425% of the total database, while those remaining were 95804 gravity observations. The statistics before and after the blunder removal are tabulated in Table 2.

Table 2. Statistics of reduced to EGM96 Bouguer gravity anomalies before and after the gross-error removal test with LSC. Unit: [mGal].

	max	min	mean	σ
$\Delta g_{B\ red}$ **(before)**	118.45	-115.23	-5.34	±26.26
$\Delta g_{B\ red}$ **(after)**	118.45	-113.40	-5.60	±26.01

2.4 Gravity database estimation

The remaining 95804 point Bouguer gravity anomalies were transformed to free-air anomalies by restoring the effect of the Bouguer plate. Finally, and in order to fill gaps in the database over Turkey, gravity anomalies from GPM98b were estimated, whilst the CAATER airborne gravity data were also implemented in the database (Olesen et al. 2003). Thus, a total number of 97466 reduced to EGM96 point free-air gravity anomalies were available.

Most databases are usually given as regular grids of mean values rather than irregularly distributed point values. The former representation is preferred due to a) the smaller size of the data files, b) the easier manipulation of the data with spectral methods, c) restrictions in the availability of the point data, etc. Therefore, the final step for the construction of the database refers to the estimation of gravity anomalies on a regular grid. For the prediction results to be more rigorous, regardless of the gridding algorithm used, the field to be interpolated has to be as smooth as possible, thus the effect of the topographic masses was removed from the data through an RTM reduction (Forsberg 1984). The Digital Terrain and Depth Model (DTDM), whose statistics are given in Table 3, has a resolution of 1 km in both latitude and longitude and was constructed by the authors at an earlier phase of the project (details available at www.gavdos.tuc.gr).

Table 3. Statistics of the 1-km DTM used for the RTM effects. Unit: [m].

	max	min	mean	σ
DTM	2394.790	-5065.950	-1562.476	±1272.917

The removal of the RTM-effects from the EGM96 reduced gravity anomalies resulted in a residual gravity anomaly field. From Table 4, which summarizes the statistics of the free-air gravity anomalies before and after the RTM reduction, it is evident that the residual field is indeed smoother since the range is reduced by 45% (139.4 mGal), the mean by 83.20% (2.82 mGal) and the σ by 40% (10.87 mGal).

To construct the final gravity grid, different gridding algorithms such as spline interpolation and weighted means were tested. But, for the gridding procedure to be rigorous we chose to grid the data using collocation. This method is obviously more time consuming compared to the other two, but provides statistically optimal results. To grid the data using LSC the correlation length and the variance of the residual field had to be computed, thus the empirical covariance function of the data has been computed and fitted to the Tscherning and Rapp model (see Figure 2). Figure 2 presents the empirical covariance functions of the gravity data before (cross) and after the RTM reduction (asterisk) as well as the one fitted to the analytical model (dot). Figure 2 strengthens the previous conclusion that the data after the RTM reduction are indeed smoother, since the variance of the data reduced and the correlation length of the field increased.

Table 4. Statistics of reduced to EGM96 free-air gravity anomalies (Δg_f) before and after the RTM reduction. Unit: [mGal].

	max	min	mean	σ
$\Delta g_{f\,red}$ **(before)**	206.08	-108.17	-3.39	±27.13
$\Delta g_{f\,red}$ **(after)**	78.99	-95.87	-0.57	±16.26

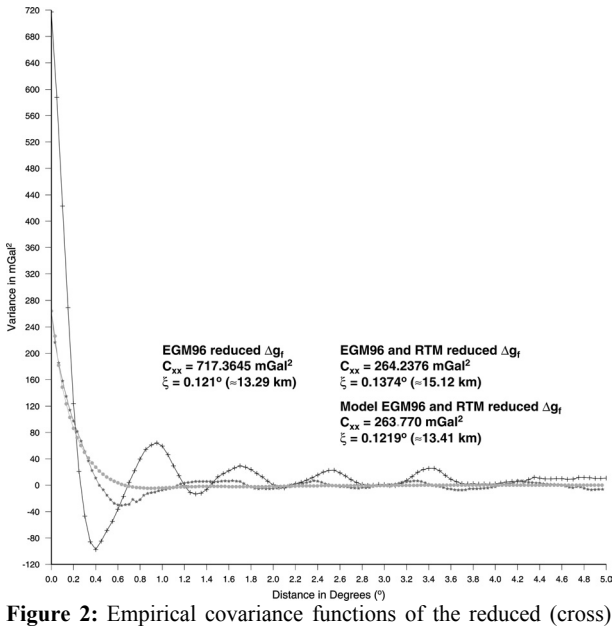

Figure 2: Empirical covariance functions of the reduced (cross) and residual (asterisk) gravity anomalies and the fitted analytical model (dot).

In this way the final residual (RTM and EGM96 reduced) free-air gravity anomaly grid has been estimated. Then, adding back the effect of the topography/bathymetry and that of the geopotential model resulted in the final 1′×1′ (corresponding to about 1.7 km spatial resolution) gravity database. Figure 3 depicts the final gravity database in the area under study, while the statistics of the gravity field over Gavdos are presented in Table 5.

Table 5. Statistics of reduced to EGM96 and final free-air gravity anomaly grid (the GAVDOS project database). Unit: [mGal].

	max	min	mean	rms	σ
$\Delta g_{f\,red}$	186.17	-104.09	-0.85	25.14	±25.12
Δg_f	230.24	-237.81	-22.16	86.07	±83.17

3 Geoid determination and validation

Using the estimated gravity database, as well as satellite altimetry data from the geodetic missions of ERS1 and GEOSAT, gravimetric, altimetric and combined geoid models have been determined for the area. In all cases the well-known remove-compute-restore method was employed, while the estimation of the gravimetric geoid was carried out using the 1D-FFT spherical Stokes convolution (Haagmans et al. 1993). The methodology followed to process the altimetric SSHs and estimate the combined ERS1 and GEOSAT altimetric geoid model is described in detail in Vergos and Sideris (2003) and Vergos et al. (2003) and will not be discussed here.

The determination of a combined gravimetric and altimetric geoid solution was performed with two methods, i.e., conventional LSC in the space domain (Moritz 1980) and the FFT-based Multiple Input Multiple Output System Theory (MIMOST) in the frequency domain (Andritsanos and Tziavos 2002). Due to a) the high-resolution of the geoid models, b) the extension of the area, and c) the fact that our main interest was over the isle of Gavdos, the combined solutions have been estimated in the inner parts of the wider area under study, to speed up the computations. Table 6 presents the statistics of the four estimated geoid models, where the gravimetric and altimetric solutions refer to the entire area under study and the combined ones to a smaller part of it. Since the LSC method is the most time-consuming one, it was limited to the area bounded between $34^o \le \varphi \le 35^o$ and $23^o \le \lambda \le 24^o$. Figures 4 and 5 depict the LSC, gravimetric and MIMOST geoid models.

Table 6. Statistics of the final geoid models for the area of Gavdos. Unit: [m].

MODEL	max	min	mean	σ
$N^{gravimetric}$	39.813	0.780	21.185	±10.352
$N^{altimetric}$	40.206	1.057	21.376	±10.484
N^{MIMOST}	37.733	6.168	2.899	±9.127
N^{LSC}	25.638	9.857	16.867	±3.951

The validation of the estimated geoid models was performed through comparisons with stacked T/P SSHs

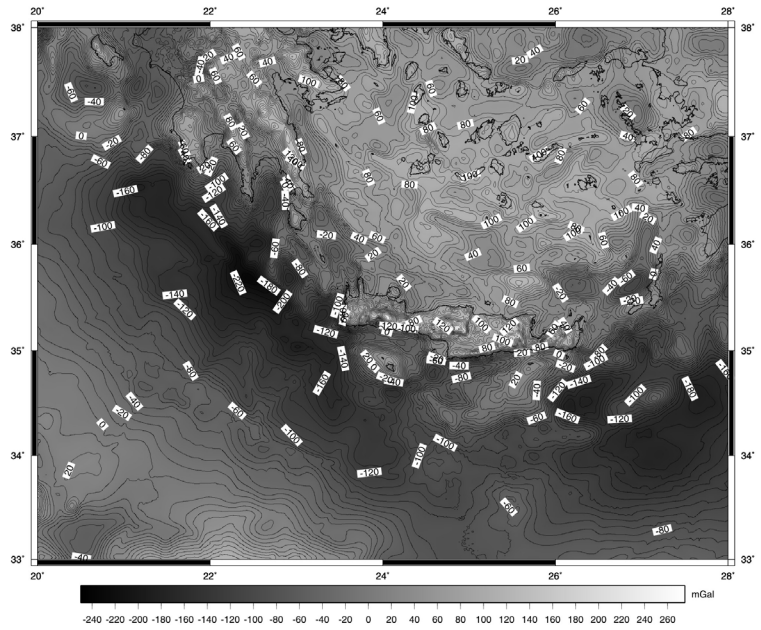

Figure 3: The final free-air gravity database in the area under study.

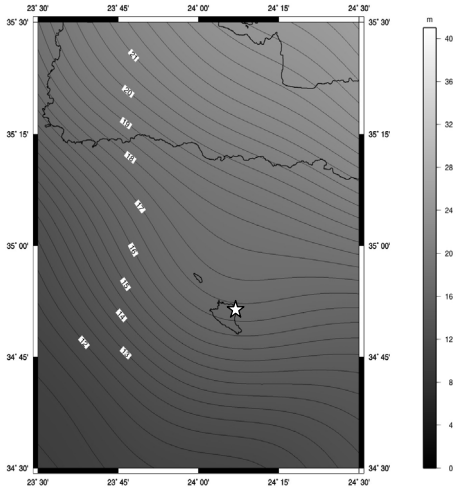

Figure 4: LSC combined geoid model for the area of Gavdos. (the asterisk shows the Karave TG station)

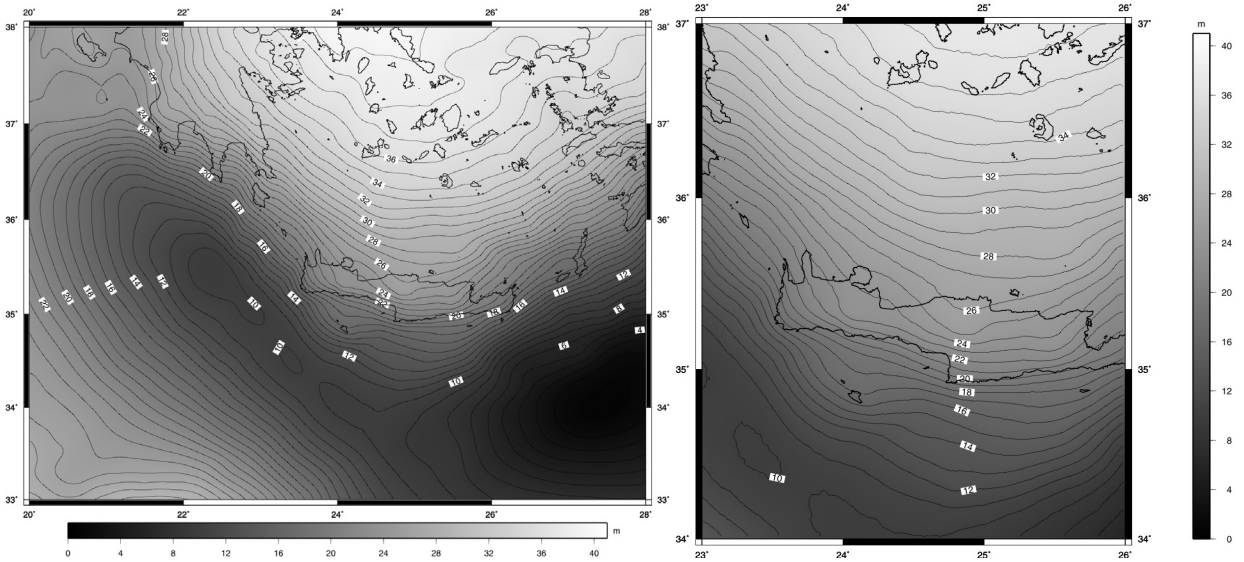

Figure 5: Gravimetric (left) and MIMOST (right) geoid models for the area of Gavdos.

spanning over nine years of the satellite mission (1993 – 2001). Furthermore, geoid heights from each model have been predicted for the Gavdos (KARAVE) tide gauge (TG) station. Table 7 summarizes the statistics of the comparisons with T/P (standard deviations only) after the fit of the differences with a 4-parameter transformation model as well as the estimated geoid heights at the TG station. No results for the comparison between the LSC geoid and T/P are presented, since the satellite points within the LSC solution are very few and would lead to over-optimistic outcomes. In Table 7, N^i refers to the geoid heights from the different models estimated, N^{TG} to the predicted height at the Karave TG station and $\sigma_{N^{TG}}$ to the accuracy of the latter. From the statistics, it can be concluded that all estimated geoid models are consistent to each other since the geoid height at the TG varies within 4 cm in the worst case. As far as the models developed are concerned, it should be noted that the altimetric geoid is superior over purely marine areas (homogeneous coverage and high accuracy), the gravimetric should be used over land areas and close to the coastline, while the combined solutions offer the advantages of both "worlds" since they represent accurately the geoid over both marine and land areas. The MIMOST combined model, provides an agreement with the T/P SSHs at the ±12.5 cm level (1σ), which is about 6 cm better compared to the previous combined solution for the area (Andritsanos et al. 2001).

Table 7. Predicted geoid height at the Gavdos TG station from the different models and comparisons with T/P SSHs.

model	σ_N^{TP}-$_N^i$ (cm)	N^{TG} (m)	σ_N^{TG} (cm)
N^{grav}	±14.5	16.70	±1.41
N^{altim}	±8.60	16.70	±0.91
N^{MIMOST}	±12.5	16.68	±1.19
N^{LSC}	----------	16.72	±0.40

4 Conclusions

A gravity anomaly database has been created from marine, land and airborne data, towards the determination of a high-accuracy and high-resolution geoid model in Gavdos, Greece. The methodology employed was a two-step procedure, i.e., a visual inspection test followed by a least squares collocation blunder detection and removal scheme. Both tests are highly objective, since in the former, holes and spikes not so deep or steep respectively can be either removed as blunders or remain in the database. In the latter, the removal of an observation as erroneous depends solely on the selection of the data error (±5 mGal in our case) and the rejection constant *k* (2 in our case). As far as the visual inspection test is concerned, only observations that could be clearly distinguished as blunders were removed, considering that any remaining erroneous observations would be removed during the LSC test. This hypothesis was more or less ensured by a) the selection of a very strict rejection constant *k* and b) a relatively small observation error. Thus practically, if the difference between the observation and the LSC prediction was larger than ~10 mGal, the observation was removed as blunder (see Eq. 3).

For the determination of the geoid models the well-known remove-compute-restore method was employed to estimate gravimetric, altimetric and combined solutions. From the results obtained and the comparisons with stacked T/P SSHs, we can conclude that the altimetric geoid gives the most precise results and outperforms the gravimetric solution by about 6 cm. One should take into account that the estimated altimetric geoid is highly correlated with the T/P data, therefore their comparison is expected to give good results. A much better validation dataset would be GPS/Leveling geoid heights at the TG station, but such information was and still is unavailable. This difference of 6 cm is probably the quasi-stationary sea surface topography in the area, which was not removed from the altimetric observations due to the unavailability of a local QSST model and the inappropriateness of the global models in closed sea areas. Of course, the altimetric geoid is prone to errors close to the coastline and unavailable on land, therefore combined gravimetric and altimetric models were determined for the area. The latter agree at about ±12.5 cm with the T/P SSHs which is a major improvement compared to the previous geoid models for the area. Finally, the consistency between the geoid models is at the ±2 – ±4 cm level, which is considered as satisfactory.

Acknowledgement

Funding for this research was provided from the EU under contract GAVDOS: EVR1-CT-2001-40019 in the frame of the EESD-ESD-3 Fifth Framework Program (www.gavdos.tuc.gr).

References

Andritsanos VD, Tziavos IN (2002) Estimation of gravity field parameters by a multiple input/output system. Phys and Chem of the Earth, Part A 25(1): 39-46.

Andritsanos VD, Vergos GS, Tziavos IN, Pavlis EC and Mertikas SP. (2001) A High Resolution Geoid for the Establishment of the Gavdos Multi-Satellite Calibration Site. In: Sideris MG (ed) Proc of International Association of Geodesy Symposia "Gravity Geoid and Geodynamics 2000", Vol. 123. Springer - Verlag Berlin Heidelberg, pp 347-354.

Andersen OB, Knudsen P (1998) Global gravity field from ERS1 and Geosat geodetic mission altimetry. J Geophys Res 103(C4): 8129-8137.

Behrent D, Denker H, Schmidt K (1996) Digital gravity data sets for the Mediterranean Sea derived from available maps. BGI Bulletin d' information 78: 31-39.

BGI (1992) BGI Bulletin d' Information Vol 70, 71.

Casten U, Makris J (2001) Erkundung der Krustenstruktur von Kreta durch detaillierete Schwere- und Magnetfeldmessunggen. Project Report DFG: Ca 83/8-1 bis 3 Ma 719/54-1 bis 3.

Forsberg R (1984) A study of terrain corrections, density anomalies and geophysical inversion methods in gravity field modeling. Rep of the Dept of Geodetic Sci and Surv No 355 The Ohio State Univ, Columbus, Ohio.

Haagmans R, de Min E, van Gelderen M (1993) Fast evaluation of convolution integrals on the sphere using 1D FFT, and a comparison with existing methods for Stokes' integral. Manuscr Geod 18: 227-241.

Lagios E, Chailas S, Hipkin RG (1996) Newly compiled gravity and topographic data banks of Greece. Geophys J Int 126: 287-290.

Moritz H (1980) Advanced Physical Geodesy. 2nd Ed Wichmann, Karlsruhe

National Geophysical Data Center (2001) GEODAS Marine trackline geophysics – Gravity, bathymetry, seismic, geophysical data.

Olesen AV, Tziavos IN, Forsberg R (2003) New Airborne Gravity Dta Around Crete – First results from the CAATER Campaign. In: Tziavos (ed) Proc of the 3rd Meeting of the Gravity and Geoid Commission "Gravity and Geoid 2002", pp 40-44.

Tscherning CC (1991) The use of optimal estimation for gross-error detection in databases of spatially correlated data. BGI, Bulletin d' Information 68: 79-89.

Tscherning CC, Rapp (1974) Closed Covariance Expressions for Gravity Anomalies, Geoid Undulations, and Deflections of the Vertical Implied by Anomaly Degree-Variance Models. Rep of the Dept of Geodetic Sci and Surv No 208 The Ohio State Univ, Columbus, Ohio.

Vergos GS, Sideris MG (2003) Estimation of High-Precision Marine Geoid Models Off-shore Newfoundland, Eastern Canada. In: Tziavos (ed) Proc of the 3rd Meeting of the Gravity and Geoid Commission "Gravity and Geoid 2002", pp 126-131.

Vergos GS, Tziavos IN, Andritsanos VD (2003) On the Determination of Marine Geoid Models by Least Squares Collocation and Spectral Methods using Heterogeneous Data. Presented at Session G03 of the 2004 IUGG General Assembly, Sapporo, Japan, July 2-8, 2003. (accepted for publication to the conference proceedings)

Wenzel HG (1999) Global models of the gravity field of high and ultra-high resolution. In: Lecture Notes of IAG's Geoid School, Milano, Italy.